(17) Durana, J. F.; McDonald, J. D. *J. Chem. Phys.* **1977**, *64*, 2518.
(18) Shi, J.; Bernfeld, D.; Barker, J. R. *J. Chem. Phys.* **1988**, *88*, 6211.
(19) Brenner, J. D.; Barker, J. R. *Astrophys. J. (Lett.)*, in press.
(20) Gillespie, D. T. *J. Comput. Phys.* **1976**, *22*, 403; *J. Phys.* **1977**, *81*, 2340; *J. Comput. Phys.* **1978**, *28*, 395.
(21) Barker, J. R. *Chem. Phys.* **1983**, *77*, 201. Shi, J.; Barker, J. R. *Int. J. Chem. Kinet.* **1990**, *22*, 187.
(22) Stein, S. E.; Rabinovitch, B. S. *J. Chem. Phys.* **1973**, *58*, 2438.
(23) Astholz, D. C.; Troe, J.; Wieters, W. *J. Chem. Phys.* **1979**, *70*, 5107.
(24) Barker, J. R. *J. Phys. Chem.* **1987**, *91*, 3849. Toselli, B. M.; Barker, J. R. *Chem. Phys. Lett.* **1989**, *159*, 499. Toselli, B. M.; Barker, J. R. *J. Phys. Chem.* **1989**, *93*, 6578.
(25) Forst, W. *J. Phys. Chem.* **1972**, *76*, 342.
(26) Cherchneff, I.; Barker, J. R. *Astrophys. J. (Lett.)* **1989**, *341*, L21. Cherchneff, I.; Barker, J. R.; Tielens, A. G. G. M. *Astrophys. J.* **1991**, *377*, 541; *Astrophys. J.*, in press.
(27) Yerram, M. L.; Brenner, J. D.; King, K. D.; Barker, J. R. *J. Phys. Chem.* **1990**, *94*, 6341. Toselli, B. M.; Barker, J. R. *Chem. Phys. Lett.* **1990**, *174*, 304. Toselli, B. M.; Brenner, J. D.; Yerram, M. L.; Chin, W. E.; King, K. D.; Barker, J. R. *J. Phys . Chem.* **1991**, *95*, 176. Toselli, B. M.; Barker, J. R. *J. Chem. Phys.* **1991**, *95*, 8108.
(28) Bishop, D. M.; Cheung, L. M. *J. Phys. Chem. Ref. Data* **1982**, *11*, 120.
(29) Wexler, A. S. *Appl. Spectrosc. Rev.* **1967**, *1*, 29.
(30) McMillen, D. F.; Golden, D. M. *Annu. Rev. Phys. Chem.* **1982**, *33*, 493.
(31) Warnatz, J. In *Combustion Chemistry*; Gardiner, W. C., Jr., Ed.; Springer-Verlag: Berlin, 1984; p 197.
(32) Tsang, W.; Hampson, R. F. *J. Phys. Chem. Ref. Data* **1986**, *15*, 1087.
(33) Benson, S. W.; Dobis, O.; Gonzalez, A. C. *J. Phys. Chem.* **1991**, *95*, 8423.
(34) Whitten, G. Z.; Rabinovitch, B. S. *J. Chem. Phys.* **1964**, *41*, 1883.
(35) Goodman, L.; Ozkabak, A. G.; Thakur, S. N. *J. Phys. Chem.* **1991**, *95*, 9044.
(36) Shimanouchi, T. *Natl. Stand. Ref. Data Ser., Natl. Bur. Stand. (U.S.)* **1972**, *No. 39*.
(37) Benson, S. W. *Thermochemical Kinetics*, 2nd ed.; Wiley: New York, 1976.
(38) Kiefer, J. H.; Mizerka, L. J.; Patel, M. R.; Wei, H.-C. *J. Phys. Chem.* **1985**, *89*, 2013.
(39) Hsu, D. S. Y.; Lin, C. Y.; Lin, M. C. *Symp. (Int.) Combust. [Proc.]* **1985**, *20*, 623.
(40) Rao, V. S.; Skinner, G. B. *J. Phys. Chem.* **1988**, *92*, 2442.
(41) Toselli, B. M.; Barker, J. R. *J. Phys. Chem.*, in press.
(42) Pamidimukkala, K. M.; Kern, R. D.; Patel, M. R.; Wei, H. C.; Kiefer, J. K. *J. Phys. Chem.* **1987**, *91*, 2148.
(43) Brand, U.; Hippler, H.; Lindemann, L.; Troe, J. *J. Phys. Chem.* **1990**, *94*, 6305.

Thermal Decomposition of 5-Methylisoxazole. Experimental and Modeling Study

Assa Lifshitz* and Dror Wohlfeiler†

Department of Physical Chemistry, The Hebrew University, Jerusalem 91904, Israel
(Received: February 18, 1992; In Final Form: May 14, 1992)

The thermal decomposition of 5-methylisoxazole was studied behind reflected shocks in a pressurized driver single-pulse shock tube over the temperature range 850–1075 K and overall densities of $\sim 2.5 \times 10^{-5}$ mol/cm^3. Propionitrile and carbon monoxide are the major decomposition products, followed by ethane, methane, acetonitrile, and hydrogen cyanide. There is no effect of large quantities of toluene ([toluene]/[5-methylisoxazole] $\sim$ 10) on the concentrations of propionitrile and acetonitrile, indicating that no radical chains are involved in their production. It is suggested that the formation of C_2H_5CN and CO in 5-methylisoxazole involves an N–O bond cleavage in the 1,2-position, a methyl group shift from position 5 to 4, and a rupture of the C(4)–C(5) bond with the removal of carbon monoxide from the ring: 5,m-isox $\rightarrow$ C_2H_5CN + CO (1). In contradiction to findings in isoxazole, this process requires a very large N–O bond stretch which results in a very loose transition state corresponding to a biradical mechanism. The rate constant for this reaction is $k_1 = 10^{17.76} \exp(-70 \times 10^3/RT)$ s^{-1} where R is expressed in units of cal/(K mol). The presence of ethane and methane in the postshock mixtures indicates the presence of methyl radicals in the hot phase. It is suggested that the formation of methyl radicals involves the same N–O bond cleavage as in reaction 1 but without the methyl group shift: 5,m-isox $\rightarrow$ $CH_2CN^\bullet$ + $CH_3CO^\bullet$ (2) followed by $CH_3CO^\bullet \rightarrow CH_3^\bullet$ + CO (3). This is an endothermic reaction which proceeds at a lower rate that reaction 1 but at a much higher rate than a direct methyl group ejection from the ring.

Introduction

We have recently published a detailed investigation on the decomposition of isoxazole behind reflected shocks in a single-pulse shock tube.[1] On the basis of the experimental findings (including tests in the presence of free radical scavengers) and on thermochemical considerations, we suggested a reaction mechanism, constructed a kinetic scheme, and performed computer simulation with good agreement between the computed and experimental results.

Isoxazole is isoelectronic to furan. Although it is kinetically much less stable than the latter, its thermal reactions, that take place at much lower temperatures, are very similar to those occurring in furan.[2] Products with a –C≡CH group in furan are replaced by –C≡N group in isoxazole. Thus, CH_3–C≡CH which is the main product in the decomposition of furan is replaced by $CH_3C{\equiv}N$ which is the main product in isoxazole. This is true also for other products.

5-Methylisoxazole is another member of the isoxazole family. It is isoelectronic with 5-methylfuran. In view of the identical ring structures it is expected that these two molecules will show similar reaction patterns in their decompositions, as isoxazole and furan do. Owing to the weak N–O bond in the ring, a low kinetic stability, and thus decomposition at relatively low temperatures, is expected. It is believed also that the stretching of this bond will be the first step in the decomposition.

It would be of great interest therefore to compare the thermal reactions and the kinetic stability 5-methylisoxazole to those of 5-methylfuran on one hand and to isoxazole on the other hand and to observe similarities and differences.

As far as we are aware, the decomposition of 5-methylisoxazole has never been studied in the past. It is expected that the results obtained in this investigation will help to establish a decomposition mechanism and to construct a kinetic scheme for computer simulation.

Experimental Section

Apparatus. The decomposition of 5-methylisoxazole was studied behind reflected shock waves in a single-pulse shock tube using the same technique which was used in the study of isoxazole decomposition. It will be described here only very briefly. The tube is made of 52-mm-i.d. stainless steel tubing with 4-m driven

† In partial fulfillment of the requirements for a Ph.D. Thesis to be submitted to the Senate of the Hebrew University by D.W.

0022-3654/92/2096-7367$03.00/0

section, 2.7-m driver section, and a 36-L dump tank. The driver section could be shortened in small steps in order to tune for the best cooling conditions. The driver section was separated from the driver by "Mylar" polyester film of various thickness depending upon the desired shock strength. Prior to performing the experiments, we pumped the tube down to approximately 2×10^{-5} Torr and then filled it with 180–120 Torr of the reaction mixture. After firing the shock, gas samples were withdrawn from the end block of the driven section and were analyzed by gas chromatography using flame ionization and nitrogen phosphor detectors.

A more detailed description of the single pulse shock tube and its mode of operation have been described in detail in previous publications.[3]

Reflected shock temperatures were calculated from the extent of conversion of 2-chloropropane to propylene and hydrochloric acid ($A = 10^{13.8}$ s^{-1}, $E = 50.87$ kcal/mol).[4] This internal standard served as a chemical thermometer in the present investigation. The reflected shock temperatures were calculated using the following equation

$$T_{ref} = -(E/R)/\ln\left\{-\frac{1}{At}\ln(1-\chi)\right\} \qquad (I)$$

where t is the reaction dwell time and χ is the extent of decomposition defined as

$$\chi = [C_3H_6]_t/([C_3H_6]_t + [C_3H_7Cl]_t) \qquad (II)$$

and E and A are the activation energy and the preexponential factor of 2-chloropropane decomposition, respectively.

Reflected shock densities were calculated from the measured incident shock velocities using the three conservation equations and the ideal gas equation of state. The latter were measured with two high-frequency pressure transducers placed 300 mm apart near the end plate of the driven section. A third transducer placed at the center of the end plate provided measurements of the reaction dwell times (approximately 2 ms) with an accuracy of approximately 5%. Cooling rates were approximately 5×10^5 K/s.

Materials and Analysis. Reaction mixtures containing approximately 0.5% 5-methylisoxazole and 0.12% 2-chloropropane in argon were prepared and stored at 1 atm in 12-L glass bulbs. Both the bulbs and the vacuum line were pumped down to better than 10^{-5} Torr before the preparation of the mixtures.

5-Methylisoxazole, listed as 97% pure, and 2-chloropropane, listed as better than 99% pure, were obtained from Aldrich Chemical Co. None of the reaction products or any other impurity could be detected in an unshocked sample of 5-methylisoxazole. Argon was Matheson ultrahigh-purity grade, listed as 99.9995%, and helium was Matheson pure grade, listed as 99.999%. All materials were used without further purification.

Two series of gas analyses were performed on each postshock mixture. In the first series shocked samples were injected into the gas chromatograph (HP Model 5890) and were then equally divided between two $^1/_8$-in. × 3-m Porapak N columns. One column, connected to a flame ionization detector (FID), separated and quantitatively determined the reaction products without bound nitrogen. The second column, connected to a nitrogen phosphor detector (NPD), separated and quantitatively determined all the nitrogen-containing species. The initial column's temperature of 35 °C was gradually elevated to 190° C in an analysis which lasted about 55 min.

In order to combine the GC peak areas in the two columns to one list, the area under the 5-methylisoxazole peak in the FID column ($A_{5,m\text{-}isox,FID}$) was set equal to that in the NPD column ($A_{5,m\text{-}isox,NPD}$), and all the FID peaks were multiplied by the ratio $A_{5,m\text{-}isox,NPD}/A_{5,m\text{-}isox,FID}$.

The purpose of the second series of analyses was to quantitatively determine the amounts of carbon monoxide in the postshock mixtures. This was performed on a Porapak N column connected to a FID. The carbon monoxide in the samples was reduced at 400 °C to methane prior to its detection using a Chrompak methanyzer with a carrier composed of 50% hydrogen and 50% argon. Each analysis gave the ratio $[CH_4]/[CO]$. From this ratio and the known methane concentration obtained previously, the concentration of CO could be calculated. The ratio $[CH_4]/[CO]$ in a standard mixture of methane and carbon monoxide was determined periodically for calibration. A typical chromatogram of a shocked mixture of 0.5% 5-methylisoxazole in argon heated to 1048 K is shown in Figure 1 for both detectors. The peaks drawn in dashed lines are those of the internal standard and its decomposition product and are not part of the 5-methylisoxazole decomposition.

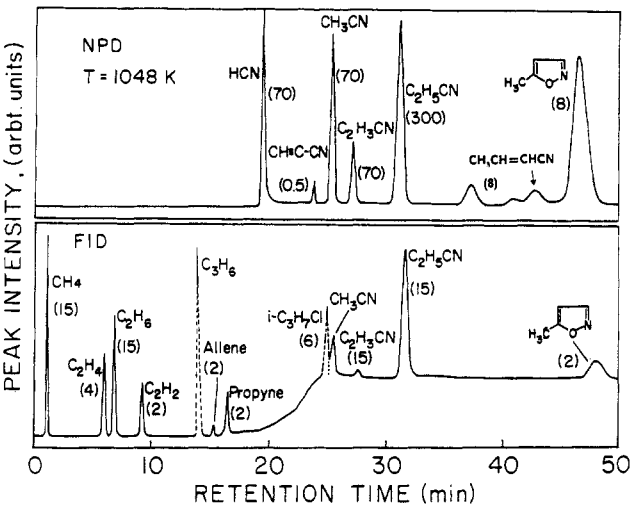

Figure 1. Gas chromatogram of a postshock mixture of 0.5% 5-methylisoxazole in argon heated to 1048 K. The chromatogram is obtained on dual 3-m Porapak N columns using FID and NPD. Carbon monoxide which is analyzed separately is not shown. (The numbers on the peaks indicate relative attenuation factors.)

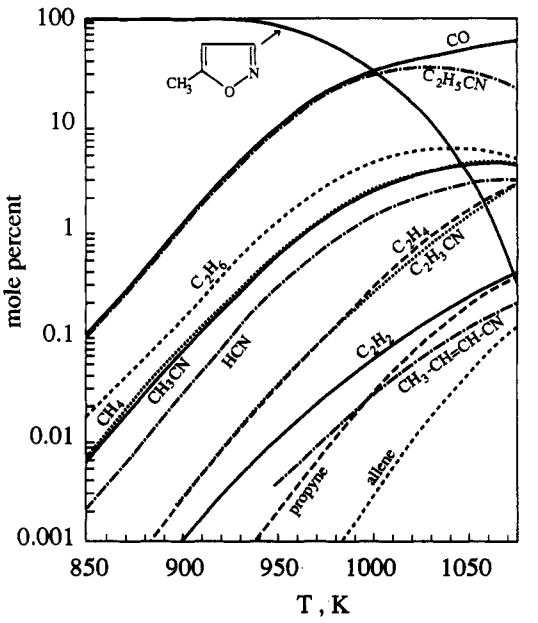

Figure 2. Distribution of reaction products as obtained in the postshock analyses. Propionitrile and carbon monoxide are the major products in the decomposition of 5-methylisoxazole.

GC peak areas were integrated with a Spectra Physics Model SP4200 computing integrator and were transferred to an IBM PC/AT for data reduction and graphical presentations.

Results

Product Distribution. The distribution of reaction products is shown in Figure 2. It is based on some 45 tests which were run with mixtures containing approximately 0.5% 5-methylisoxazole in argon at initial pressures p_1 ranging from 80 to 120 Torr, covering the temperature range 850–1075 K. Extents of pyrolysis as low as a few thousands of one percent were determined.

TABLE I: Experimental Conditions and Product Distribution in Percent

T_{ref} (K)	t^a	$C_{ref} \times 10^{5\,b}$	5,m-isox	C_2H_5CN	CO	C_2H_6	CH_4	CH_3CN	HCN	C_2H_4	C_2H_2	C_2H_3CN
810	2.47	2.39	99.927	0.014	0.050							
845	2.32	2.28	99.763	0.092	0.106	0.011	0.0056		0.0030			
860	2.26	2.23	99.609	0.191	0.120	0.028	0.014		0.0063			
882	2.06	2.24	99.068	0.509	0.353	0.054	0.022		0.0088			
910	2.00	2.24	95.592	1.95	1.85	0.252	0.124	0.0706	0.0361	0.002		
934	2.05	2.24	89.480	3.90	3.39	0.53	0.26	0.29	1.99	0.011	0.007	0.007
988	2.28	2.12	42.078	26.41	22.55	3.28	2.13	2.03	1.06	0.176	0.039	0.229
1011	2.00	2.38	30.065	30.59	28.40	3.71	0.85	2.33	1.35	0.237	0.054	0.375
1029	2.00	2.42	12.580	34.96	36.27	4.74	4.32	3.75	1.82	0.378	0.072	0.829
1058	2.04	2.22	1.132	28.03	47.62	5.05	7.44	3.30	2.57	1.473	0.218	2.517

[a] In units of ms. [b] In units of $cm^3\ mol^{-1}$.

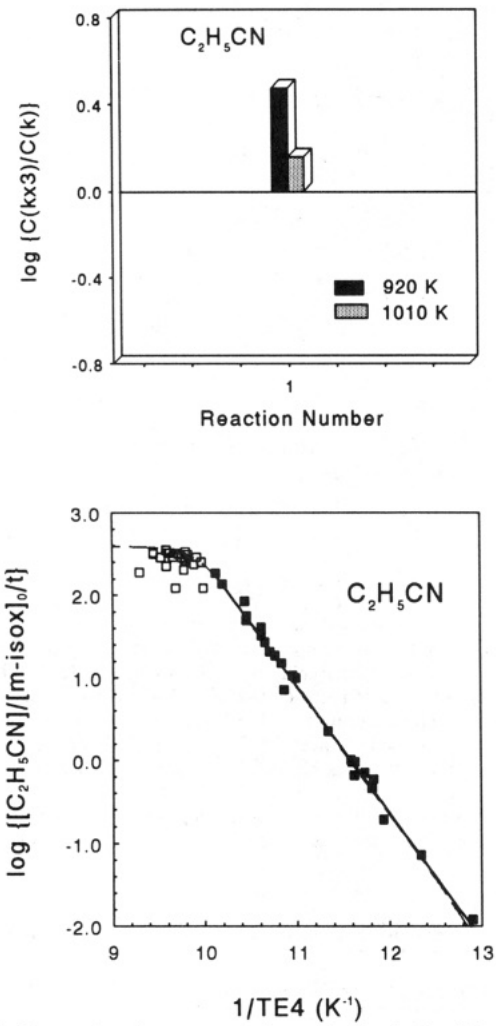

Figure 3. Comparison between experimental and calculated first-order rate constants of formation of propionitrile $\{[C_2H_5CN]_t/[5\text{-methylisoxazole}]_0\}/t$ (bottom) and the sensitivity analysis for its production (top). The solid line combining the points up to 1000 K (■) gives the Arrhenius rate parameters for the unimolecular formation of propionitrile. The broken line (coincides with the solid line) represents the best fit through the points which are calculated at 25 K intervals using the reaction scheme listed in Table III. Sensitivity analysis is shown at 920 and 1010 K. It gives the percent change in the concentration of propionitrile resulting from a factor of 3 increase in the rate constant. Only reaction 1 has an effect larger than 15%.

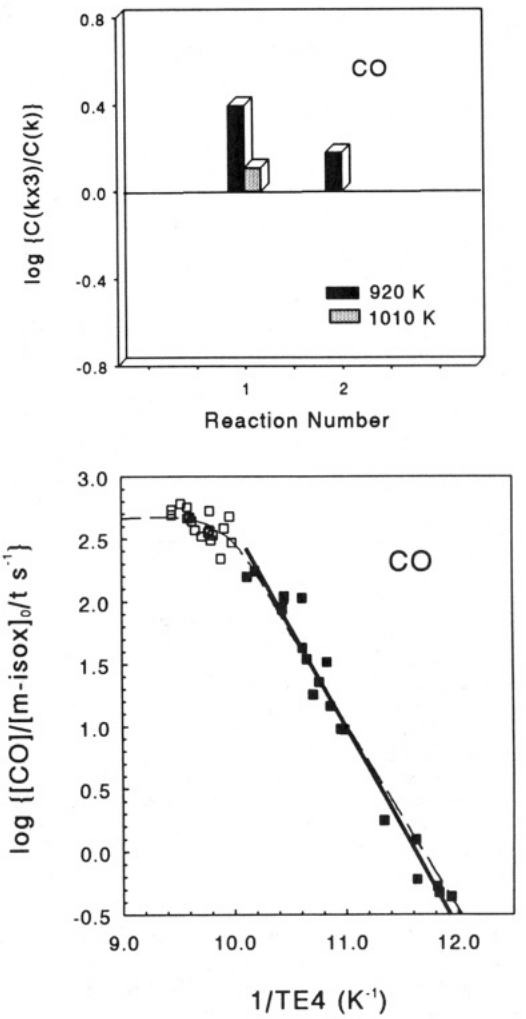

Figure 4. Comparison between experimental and calculated first-order rate constants of formation of carbon monoxide $\{[CO]_t/[5\text{-methylisoxazole}]_0\}/t$ (bottom) and the sensitivity analysis for its production (top). The solid line combining the points up to 1000 K (■) gives the Arrhenius rate parameters for the formation of carbon monoxide. The broken line (almost coincides with the solid line) represents the best fit through the points which are calculated at 25 K intervals using the reaction scheme listed in Table III. Sensitivity analysis is shown at 920 and 1010 K. It gives the percent change in the concentration of carbon monoxide resulting from a factor of 3 increase in the rate constant. The production rate of carbon monoxide is sensitive to reactions 1 and 2.

Details of the experimental conditions and the distribution of reaction products in several representative tests are given in Table I. The table shows the temperature behind the reflected shock T_5 as calculated from the conversion of the internal standard, the reaction dwell time in milliseconds, the overall density behind the reflected shock C_5 (in units of mol/cm^3), and the mole percent of the various reaction products in the mixture ($100\ C_i/\sum C_i$) as obtained from the postshock analyses. The percent of a given product shown in Table I corresponds to its mole percent, irrespective of the number of its carbon atoms and not including hydrogen and argon.

As can readily be seen, carbon monoxide and propionitrile are formed in practically equal amounts and are the major reaction products. They are followed by ethane and methane as products without bound nitrogen and acetonitrile and hydrogen cyanide as products with bound nitrogen. Small quantities of ethylene, acrylonitrile, acetylene, allene, and methylacetylene were also found in the mixtures. Succinonitrile ($CNCH_2CH_2CN$), which

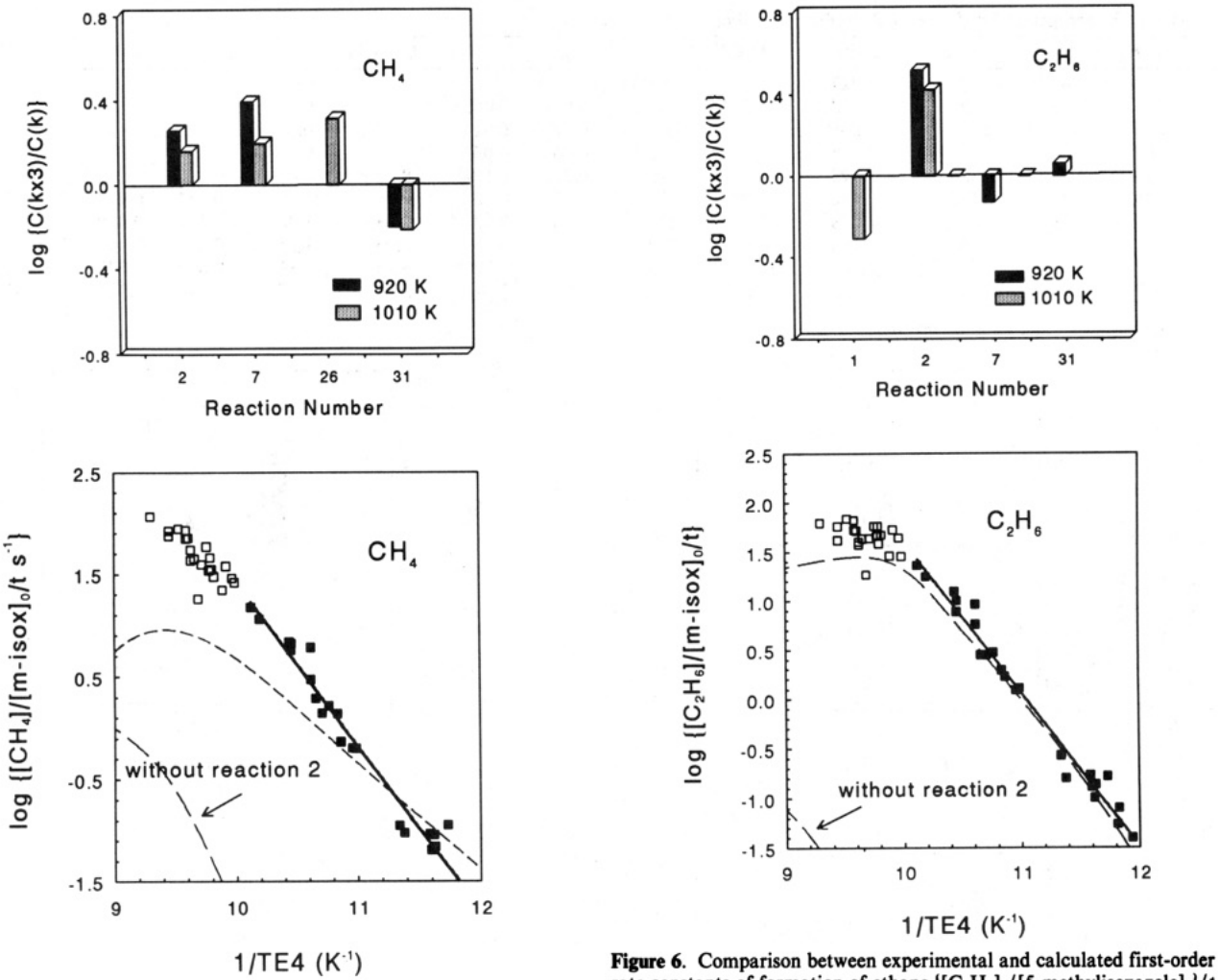

Figure 5. Comparison between experimental and calculated first-order rate constants of formation of methane $\{[CH_4]_t/[5\text{-methylisoxazole}]_0\}/t$ (bottom) and the sensitivity analysis for its production (top). The solid line combining the points up to 1000 K (■) gives the Arrhenius rate parameters for methane formation. The broken line represents the best fit through the points which are calculated at 25 K intervals using the reaction scheme listed in Table III. The agreement is not satisfactory. Sensitivity analysis is shown at 920 and 1010 K. It gives the percent change in the concentration of methane resulting from a factor of 3 increase in the rate constant.

Figure 6. Comparison between experimental and calculated first-order rate constants of formation of ethane $\{[C_2H_6]_t/[5\text{-methylisoxazole}]_0\}/t$ (bottom) and the sensitivity analysis for its production (top). The solid line combining the points up to 1000 K (■) gives the Arrhenius rate parameters for ethane formation. The broken line represents the best fit through the points which are calculated at 25 K intervals using the reaction scheme listed in Table III. The agreement is very good. Sensitivity analysis is shown at 920 and 1010 K. It gives the percent change in the concentration of ethane resulting from a factor of 3 increase in the rate constant. Only reactions which show an effect larger than 15% are listed.

is believed to be formed by $CH_2CN^{\bullet}$ recombination, could not be recovered from the postshock mixtures.

Arrhenius Parameters. Figures 3–11 show first-order rate constants for the production of the decomposition products, defined as

$$k_{1st}(\text{product}_i) = \{C_5(\text{product}_i)_t/[5,\text{m-isox}]_0\}/t \qquad \text{(III)}$$

plotted (in units of s^{-1}) against reciprocal temperature. The squares are the experimental data points. The solid lines are the best fit through the data points below 1000 K (■), and the dashed lines are the best fit through the calculated values at 25 K intervals using a reaction scheme which is listed in Table III.

According to this definition, the Y axis in these figures corresponds to a first-order rate constant. It would be a true constant for products which are formed directly from the reactant in a unimolecular process. It would be a pseudo-first-order rate constant for those whose production requires more than one step. As can be seen, in this particular presentation, the data points "bend" toward the high-temperature end. This behavior, which can be seen also in the modeling calculations, is due to depletion of the reactant at high extents of reaction (high temperatures) but also owing to further decomposition of the product (mainly by free radical attack).

TABLE II: First-Order Arrhenius Parameters for Product Formation

compd	log A/s^{-1}	E, kcal/mol	compd	log A/s^{-1}	E, kcal/mol
5,m-isox[a]	18.46	73	CH_4	17.44	73
C_2H_5CN	17.76	70	C_2H_3CN	25.04	112
CO	17.57	69	C_2H_2	17.44	81
HCN	17.47	75	C_2H_4	22.38	100
CH_3CN	17.59	75	C_2H_6	17.10	71

[a] First-order rate constant for the overall decomposition of 5-methylisoxazole.

Values of E in units of kcal/mol which are obtained from the slopes of these log k vs $1/T$ lines and their corresponding preexponential factors are summarized in Table II. These values were obtained from data points below 1000 K where the total conversion of the reactant did not exceed 50% and before curvatures in the plots began to appear.

Figure 12 shows the first-order rate constant for the overall decomposition of 5-methylisoxazole calculated from the relation $k_{total} = -\ln\{[5\text{-methylisoxazole}]_t/[5\text{-methylisoxazole}]_0\}/t$. The value obtained is $k_{total} = 10^{18.46}\exp(-73 \times 10^3/RT)\ s^{-1}$ where R is expressed in units of cal/(K mol). Expressing k_{total} as a first-order rate constant does not imply that the pyrolysis of

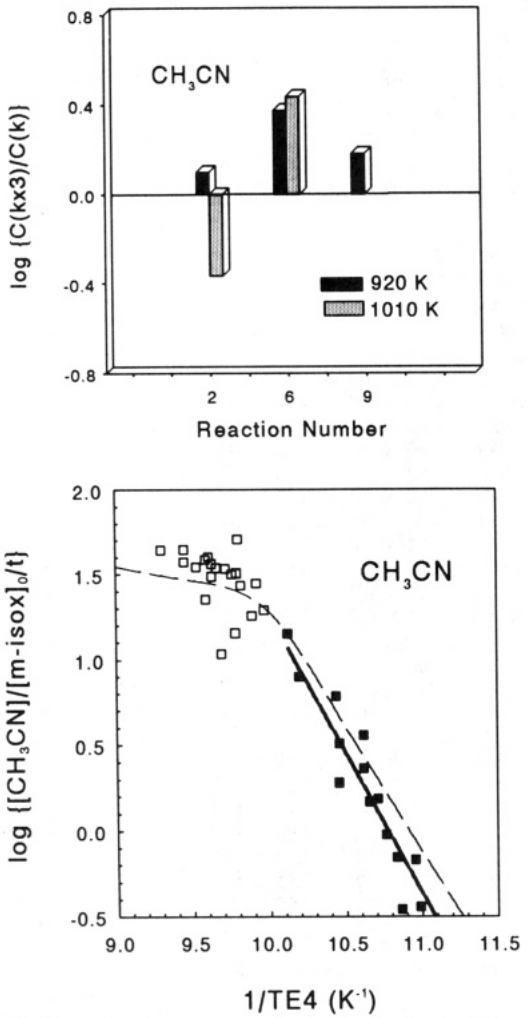

Figure 7. Comparison between experimental and calculated first-order rate constants of formation of acetonitrile $\{[CH_3CN]_t/[5\text{-methylisoxazole}]_0\}/t$ (bottom) and the sensitivity analysis for its production (top). The solid line combining the points up to 1000 K (■) gives the Arrhenius rate parameters for the formation of acetonitrile. The broken line represents the best fit through the points which are calculated at 25 K intervals using the reaction scheme listed in Table III. The agreement is very good. Sensitivity analysis is shown at 920 and 1010 K. It gives the percent change in the concentration of acetonitrile resulting from a factor of 3 increase in the rate constant. Acetonitrile is produced mainly by reaction 6. It is depleted by free radical attack mainly at high temperatures and is thus sensitive to reaction 2 which initiates free radicals.

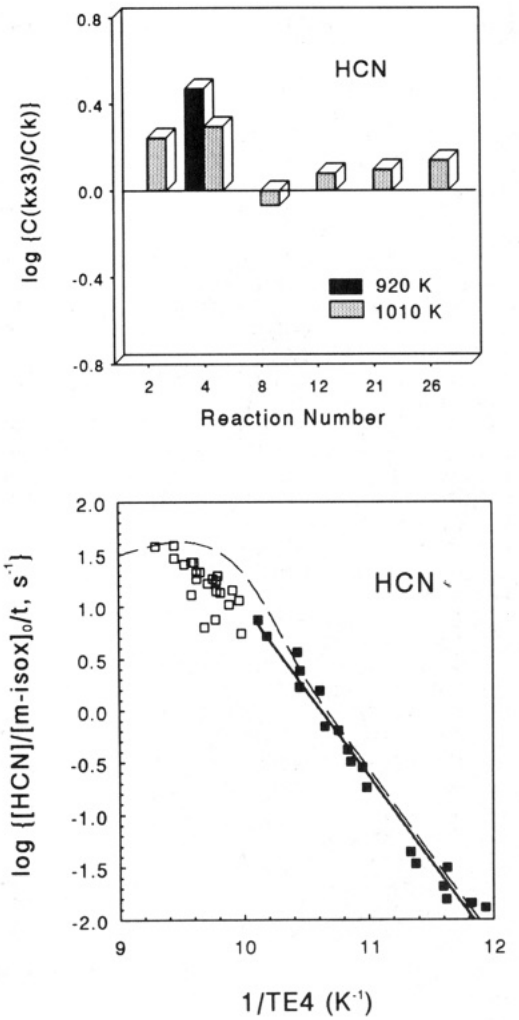

Figure 8. Comparison between experimental and calculated first-order rate constants of formation of hydrogen cyanide $\{[HCN]_t/[5\text{-methylisoxazole}]_0\}/t$ (bottom) and the sensitivity analysis for its production (top). The solid line combining the points up to 1000 K (■) gives the Arrhenius rate parameters for the formation of hydrogen cyanide. The broken line represents the best fit through the points which are calculated at 25 K intervals using the reaction scheme listed in Table III. The agreement is very good. Sensitivity analysis is shown at 920 and 1010 K. It gives the percent change in the concentration of hydrogen cyanide resulting from a factor of 3 increase in the rate constant.

5-methylisoxazole obeys, under the conditions of the present experiments, a first-order reaction. It is a good way, however, to show the overall decomposition rate and its temperature dependence. As will be discussed later, the decomposition is composed of a large number of elementary reactions involving unimolecular dissociations as well as free radical reactions.

Discussion

Reaction Mechanism. *Unimolecular Ring Opening.* As can be seen in Figure 2, the major products in the decomposition of 5-methylisoxazole are propionitrile and carbon monoxide. In order to examine the extent of free-radical involvement, if any, in their production we have compared the production rate of propionitrile in the absence and presence of large excess toluene over a wide temperature range. The results of these experiments are shown in Figure 13 where ratios [propionitrile]/[5-methylisoxazole] are plotted (in arbitrary units) against reciprocal temperature. As can be seen the rates are unaffected by toluene, and it is thus reasonable to assume that propionitrile is produced by a unimolecular decomposition of 5-methylisoxazole. This process takes place by (1) breaking the N–O bond in the ring, (2) methyl group shift from position 5 to position 4, and (3) rupture of the C(4)–C(5) bond with the removal of carbon monoxide from the ring:

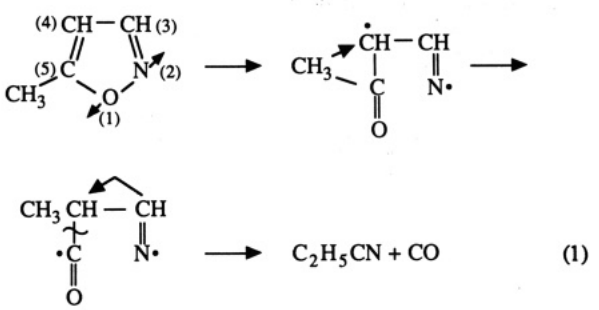

(1)

The question as to whether this is a concerted process where the three reactions occur simultaneously or whether this is more like a biradical process can be answered by examining the values of the Arrhenius parameters for the reaction. This is shown in Figures 3 and 4 where the first-order rate constants for the formation of propionitrile and carbon monoxide are plotted against reciprocal temperature. The slopes of these lines (~70 kcal/mol), which are very close to the N–O bond dissociation energy in the

TABLE III: Reaction Scheme for the Decomposition of 5-Methylisoxazole[a]

reaction	A	n	E	k_f (950 K)	k_r (950 K)	ΔH_r° (1000 K)	source
1. 5,m-isox → C_2H_5CN + CO	6.82×10^{17}	0	70487	4.50×10^{1}	3.71×10^{-11}	−23.2	this work
2. 5,m-isox → CH_3CO + CH_2CN	7.81×10^{14}	0	60000	1.32×10^{1}	1.09×10^{4}	49.5	this work
3. CH_3CO → CH_3 + CO	6.79×10^{12}	0	16890	9.01×10^{8}	6.80×10^{9}	11.2	NIST
4. 5,m-isox → HCN + CH_3CHCO	6.29×10^{16}	0	72308	1.59×10^{0}	3.73×10^{-8}	−0.33	this work
5. CH_3CHCO → C_2H_4 + CO	3.00×10^{13}	0	50000	9.99×10^{1}	4.36×10^{2}	8.70	est
6. 5,m-isox → CH_2CO + CH_3CN	4.18×10^{17}	0	74551	3.22×10^{0}	1.21×10^{-7}	−2.23	this work
7. 5,m-isox + CH_3 → CH_4 + $C_3H_2NO(CH_2)$	1.50×10^{12}	0	10000	7.60×10^{9}	4.22×10^{5}	−19.4	est
8. 5,m-isox + H → H_2 + $C_3H_2NO(CH_2)$	5.00×10^{13}	0	9000	4.30×10^{11}	1.19×10^{6}	−18.2	est
9. 5,m-isox + CH_2CN → $C_3H_2NO(CH_2)$ + CH_3CN	4.00×10^{11}	0	10000	2.03×10^{9}	1.59×10^{9}	0.99	est
10. 5,m-isox → C_3H_2NO + CH_3	5.00×10^{16}	0	98000	1.59×10^{-6}	5.67×10^{10}	99.5	this work
11. C_3H_2NO → CO + CH_2CN	7.08×10^{12}	0	43470	7.44×10^{2}	1.31×10^{-10}	−38.8	est
12. $C_3H_2NO(CH_2)$ → C_2H_3 + CO + HCN	1.23×10^{15}	0	60000	2.07×10^{1}	2.94×10^{-1}	30.2	est
13. $C_3H_2NO(CH_2)$ → CO + C_2H_4CN	1.36×10^{17}	0	70000	1.16×10^{1}	4.60×10^{-8}	−9.24	est
14. CH_3CN + H → CH_3 + HCN	1.01×10^{13}	0	2000	3.52×10^{12}	1.02×10^{9}	−7.93	est
15. CH_3CN + CH_3 → CH_4 + CH_2CN	5.00×10^{11}	0	9000	4.30×10^{9}	1.23×10^{7}	−13.4	est
16. CH_3CN + H → H_2 + CH_2CN	2.61×10^{13}	0	8000	3.80×10^{11}	5.43×10^{7}	−12.2	est
17. CH_2CN + C_2H_5CN → C_2H_4CN + CH_3CN	4.00×10^{11}	0	13330	3.48×10^{8}	3.25×10^{10}	8.00	est
18. H + CH_2CN → CH_3CN	4.86×10^{12}	0	0	4.86×10^{12}	1.50×10^{-7}	−94.0	est
19. CH_2CN + CH_2CN → $C_4H_4N_2$	1.23×10^{14}	−0.50	0	3.97×10^{12}	1.35×10^{0}	−67.0	est
20. $C_4H_4N_2$ → C_2H_3CN + HCN	1.14×10^{13}	0	68000	2.79×10^{-3}	4.67×10^{4}	39.1	est
21. H + $C_4H_4N_2$ → C_2H_4CN + HCN	2.10×10^{13}	0	2000	7.30×10^{12}	2.96×10^{12}	1.11	est
22. C_2H_4CN → C_2H_3CN + H	9.30×10^{13}	0	38400	1.42×10^{5}	5.87×10^{12}	38.0	est
23. C_2H_3CN + H → HCN + C_2H_3	3.01×10^{12}	0	6500	9.70×10^{10}	8.41×10^{9}	1.41	est
24. CH_3 + CH_2CN → C_2H_5CN	2.00×10^{12}	0	0	2.00×10^{12}	2.64×10^{-4}	−84.0	est
25. C_2H_5CN + H → C_2H_4CN + H_2	1.30×10^{13}	0	10000	6.58×10^{10}	8.77×10^{8}	−4.21	est
26. C_2H_5CN + CH_3 → C_2H_4CN + CH_4	3.00×10^{12}	0	9000	2.58×10^{10}	6.88×10^{9}	−5.43	est
27. C_2H_5CN + H → C_2H_5 + HCN	2.80×10^{12}	0	5000	1.99×10^{11}	8.72×10^{7}	−6.35	est
28. H + C_2H_4CN → C_2H_5CN	1.00×10^{13}	0	0	1.00×10^{13}	3.31×10^{-9}	−102	est
29. CH_3 + CH_3 → C_2H_5 + H	2.80×10^{13}	0	13593	2.12×10^{10}	1.37×10^{14}	11.6	6
30. C_2H_5 → C_2H_4 + H	4.80×10^{9}	1.19	38205	2.86×10^{4}	8.12×10^{12}	38.0	NIST
31. CH_3 + CH_3 → C_2H_6	2.50×10^{13}	0	0	2.50×10^{13}	3.98×10^{-4}	−90.8	NIST
32. C_2H_3 + Ar → C_2H_2 + H + Ar	3.00×10^{15}	0	32030	1.33×10^{8}	3.67×10^{16}	40.7	NIST
33. CH_3 + H_2 → CH_4 + H	6.46×10^{2}	3.00	7700	9.51×10^{9}	1.91×10^{11}	−1.22	NIST
34. H + C_2H_4 → C_2H_3 + H_2	5.01×10^{13}	0	8000	7.30×10^{11}	2.80×10^{11}	3.60	NIST
35. 5,m-isox → H + $C_3H_2NO(CH_2)$	1.00×10^{14}	0	88000	6.30×10^{7}	3.96×10^{11}	−88.0	NIST

[a] ΔH°_r are expressed in units of kcal/mol. Rate constants are expressed as $k \rightarrow AT^n \exp(-E/RT)$ in units of cm^3, s, mol, cal.

ring, indicate that the N–O bond in the transition state must be practically broken before C(4) acquires the free-radical character needed to allow a methyl group to migrate from C(5). A broken bond will result in a very loose biradical transition structure and thus a high preexponential factor. The value of $A = (4.6 \pm 1.4) \times 10^{17}$ as the average for the production of propionitrile and carbon monoxide is indeed extremely high. It should be mentioned that the formation of the biradical, which is the first step in the sequence of events represented by reaction 1, is rate determining. The mechanism of the second and third steps, which have much lower barriers, do not affect the nature of the overall reaction.

A process similar to the one described here was suggested also for the decomposition of isoxazole,[1] except that in isoxazole *H atom* migrates from position 5 to 4 instead of a methyl group and *acetonitrile* rather than propionitrile is formed together with carbon monoxide.

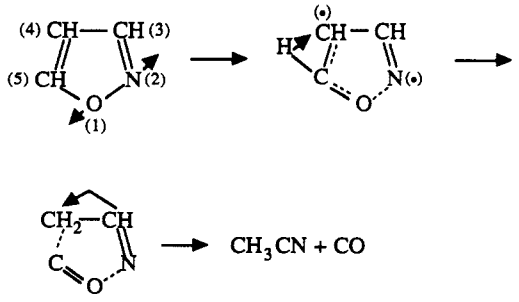

$CH_3CN + CO$ (1_{isox})

Although these processes and their transition states are very similar, the distribution of their bond lengths is very different. In order that a migration of CH_3 from position 5 to 4 in 5-methylisoxazole will take place, a large stretch of the N–O bond is required. The migration of H atom in isoxazole, on the other hand, will take place with minimal "sensitization" of position 4 and will thus require only a very small stretch of the bond. This expresses itself by a very low activation energy and a very low preexponential factor.

Figure 14 shows, for comparison, two Arrhenius plots, the production of acetonitrile from isoxazole and the production of propionitrile from 5-methylisoxazole. The large difference in the Arrhenius parameters and in the activation energies can be readily seen.

Free-Radical Initiation Reactions. The relatively large concentrations of methane and ethane and the presence of molecules such as acrylonitrile and others, in the postshock mixtures, clearly indicate that free radicals do play a role in the overall decomposition of 5-methylisoxazole and the question of their initiation should be addressed. Normally, the presence of a methyl group attached to a ring will suggest that the initiation reaction would be the rupture of the methyl group from the ring or a rupture of a hydrogen atom from the methyl group. However, over the temperature range of the present experiment these two processes are extremely slow and cannot account for the large concentrations of methane and ethane which were recovered from the postshock mixtures. When the ejection of a methyl group from the ring (reaction 10) was introduced into the kinetic scheme as the sole initiator of free radicals, only minute quantities of ethane, methane, and other products were obtained by the modeling calculations. In fact, their concentrations were orders of magnitude below their detection limit. One must therefore assume that there is another reaction that initiates free radicals in the system.

It is suggested that the initiation of free radicals in 5-methylisoxazole takes place in a mechanism similar to the one that was suggested previously for isoxazole. The rupture of the N–O bond is followed by rupture of the C(4)–C(5) bond in the ring but *without* methyl group shift from C(5) to C(4).

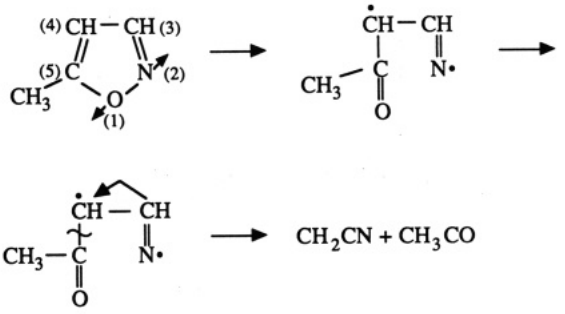

$$CH_3CO^{\bullet} \longrightarrow CH_2CN + CH_3CO \qquad (2)$$

$CH_3CO^{\bullet}$, which is generated in this process, then decomposes to yield methyl radicals and carbon monoxide. In isoxazole decomposition we assumed that the activation energy of the reaction was roughly equal to its endothermicity and adjusted the preexponential factor so as to best fit the experimental mole percents. The same considerations are being used here. They are also based on the idea that since the methyl group does not have to migrate, then the N–O bond does not necessarily have to be broken before the elimination of CH_3CO from the molecule. This will result in a tighter structure for the transition state and hence a lower preexponential factor. The value suggested for k_2 is $k_2 = 10^{14.89} \exp(-60 \times 10^3/RT)\ s^{-1}$. This value is in reasonable accord with a preexponential factor that can be expected for such a dissociation.

Acetonitrile and Hydrogen Cyanide. Figure 15 shows that there is no effect of toluene on the production rate of acetonitrile, indicating that the latter is formed from 5-methylisoxazole in a unimolecular reaction. This will require migration of a hydrogen atom from the methyl group to position 4 in the ring, regardless of whether it is a double 1,2-migration or 1,3-migration at this stage. Judging by the high activation energy and high preexponential factor for acetonitrile formation, such a process will take place after breaking the N–O bond in the ring. It is then followed by cleavage of the C(4)–C(5) bond with the formation of acetonitrile and ketene.

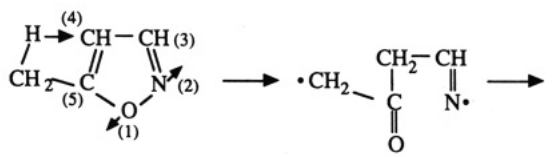

$$\bullet CH_2{-}C(=O){-}CH{=}CH{-}N\bullet \longrightarrow CH_3CN + CH_2CO \qquad (4)$$

Our results on the effect of toluene on the production rate of HCN are not very conclusive. It is believed that its production in methylisoxazole is very similar to its production in the decomposition of isoxazole, namely, breaking of the N–O bond, a methyl group shift, and rupture of the C(3)–C(4) rather than the C(4)–C(5) bond in the ring.

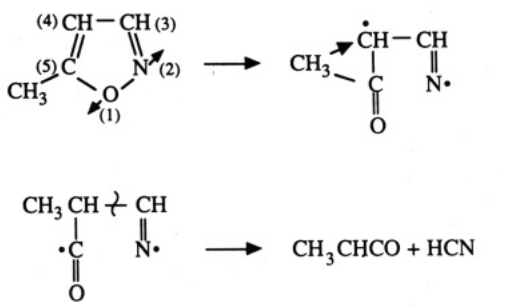

$$CH_3CH{=}C(\bullet)CO{-}N\bullet \longrightarrow CH_3CHCO + HCN \qquad (6)$$

This process also yields methylketene in addition to hydrogen cyanide. In a consecutive reaction methylketene decomposes in a concerted mechanism to carbon monoxide and ethylene and provides the main source for ethylene. Hydrogen cyanide is

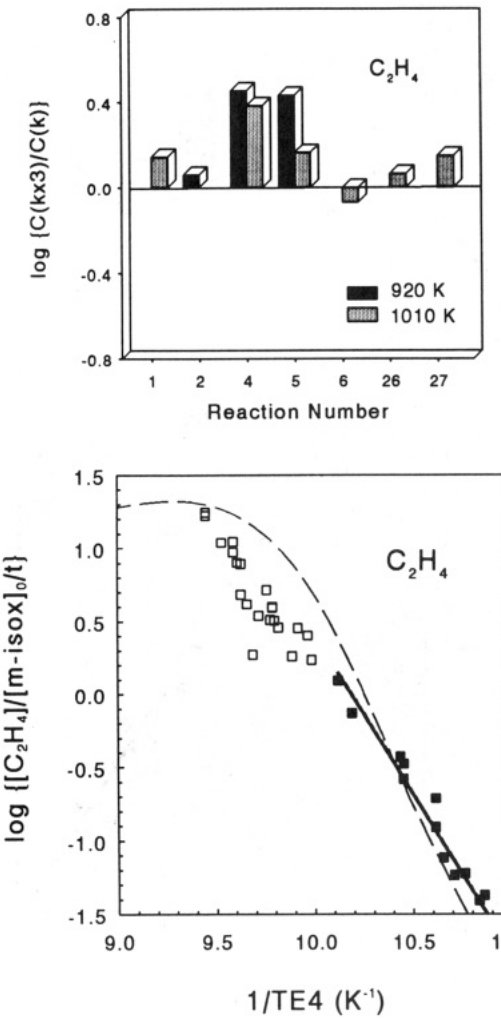

Figure 9. Comparison between experimental and calculated first-order rate constants of formation of ethylene $\{[C_2H_4]_t/[5\text{-methylisoxazole}]_0\}/t$ (bottom) and the sensitivity analysis for its production (top). The solid line combining the points up to 1000 K (■) gives the Arrhenius rate parameters for the formation of ethylene. The broken line represents the best fit through the points which are calculated at 25 K intervals using the reaction scheme listed in Table III. The calculated slope is somewhat higher than the experimental one. Sensitivity analysis is shown at 920 and 1010 K. It gives the percent change in the concentration of ethylene resulting from a factor of 3 increase in the rate constant. Ethylene is affected mainly by reactions 4 and 5.

produced also by an attack of H atoms on acetonitrile and propionitrile, particularly at high temperatures. The low concentration of hydrogen cyanide relative to propionitrile shows again that C(3)–C(4) bond cleavage in unsaturated five-member heterocyclics is considerably less favorable than cleavage of the C(4)–C(5) bond in the same molecule.[2]

Reaction Scheme and Computer Modeling. On the basis of the arguments raised above, we have constructed a kinetic scheme which describes the total decomposition of 5-methylisoxazole. The scheme contains 23 species and 35 elementary reactions. It is listed in Table III. The first three columns in the table give the three parameters A, n, and E for the forward rate constants corresponding to the reactions as they are listed in the table. The rate constants are given by $k = AT^n \exp(-E/RT)$ in units of cm^3, mol, s. Column 4 gives the values of the forward rate constants as calculated from the rate parameters at a temperature of 950 K, and column 5 shows the value for the reverse rate constants calculated from k_f and the equilibrium constants of the reactions, also at 950 K. In column 6 the standard enthalpy change at 1000 K for each reaction is given. The scheme is composed of unimolecular dissociations of the reactant molecule, unimolecular dissociations of radical intermediates, abstractions, and recombinations. The rate parameters assigned for the various unimo-

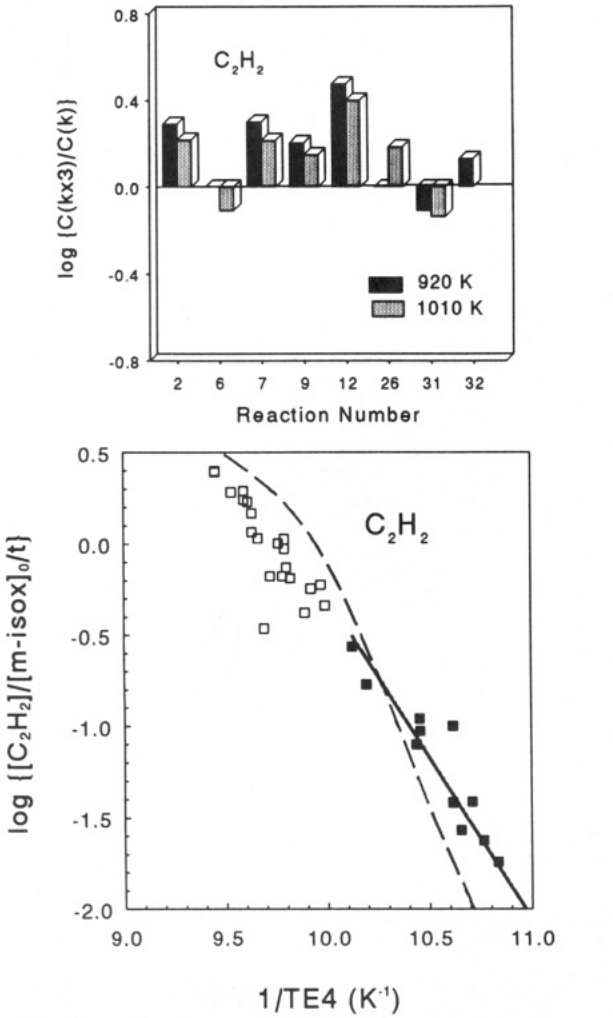

Figure 10. Comparison between experimental and calculated first-order rate constants of formation of acetylene $\{[C_2H_2]_t/[5\text{-methylisoxazole}]_0\}/t$ (bottom) and the sensitivity analysis for its production (top). The solid line combining the points up to 1000 K (■) gives the Arrhenius rate parameters for the formation of acetylene. The broken line represents the best fit through the points which are calculated at 25 K intervals using the reaction scheme listed in Table III. The calculated slope is considerably higher than what has been found experimentally. Sensitivity analysis is shown at 920 and 1010 K. It gives the percent change in the concentration of acetylene resulting from a factor of 3 increase in the rate constant. Its production rate is sensitive to a large number of reactions.

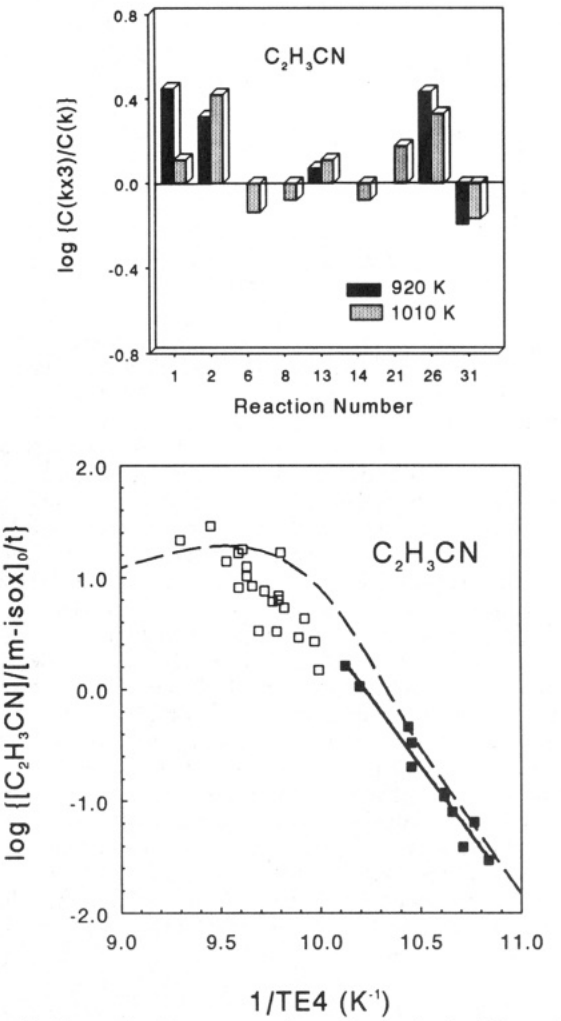

Figure 11. Comparison between experimental and calculated first-order rate constants of formation of acrylonitrile $\{[C_2H_3CN]_t/[5\text{-methylisoxazole}]_0\}/t$ (bottom) and the sensitivity analysis for its production (top). The solid line combining the points up to 1000 K (■) gives the Arrhenius rate parameters for the formation of acrylonitrile. The broken line represents the best fit through the points which are calculated at 25 K intervals using the reaction scheme listed in Table III. The agreement is good except that the calculated slope is somewhat higher than the experimental one. Sensitivity analysis is shown at 920 and 1010 K. It gives the percent change in the concentration of acrylonitrile resulting from a factor of 3 increase in the rate constant. Its production rate is sensitive to a large number of reactions.

lecular ring openings to produce propionitrile and carbon monoxide (reaction 1), methylketene and hydrogen cyanide (reaction 4), and ketene and acetonitrile (reaction 6) are based on the experimental Arrhenius plots as described previously. They are all characterized by very loose transition states and high activation energies. The activation energy for reaction 2 was taken as somewhat higher than its endothermicity, and the preexponential factor was determined according to the best fit of the data as has been discussed previously.

The Arrhenius parameters for the other reactions were either estimated or taken from the NIST Kinetic Data Base.[5] They were varied within the limits of their reported uncertainties. The Arrhenius rate parameters for each reaction that were taken from the NIST Kinetic Data Base are the best fit to a large number of entries. In view of the very large number of citations involved, they are not given as references in this article. Parameters for reactions which could not be found in available compilations were determined by comparison with similar reactions for which the rates parameters are known.

The thermodynamic properties of the species involved were taken from various literature sources.[7-10] The heat of formation of two species, $C_3H_3NO^{\bullet}$ (5-methylisoxazole after losing a methyl group) and $C_3H_3NO(CH_2)^{\bullet}$, were evaluated on the basis of the >C–CH_3 and the $C_3H_3NO(CH_2$–H) bond energies which were taken as 100 and 88 kcal/mol, respectively. The computer program available to us can perform sensitivity analysis with respect to variations (or rather uncertainties) in the $\Delta H_f°$ of the species. In several tests that were performed we found that the results of the simulation were very insensitive to these values and thus consider them adequate.

Figures 3–11 show comparisons between first-order rate constants of production of the products as defined by eq III and the calculations using the reaction scheme given in Table III. The points in the figures are experimental, and the dashed lines are the best fit through the calculations at 25 K intervals.

The figures also show sensitivity analyses for the formation of these products calculated at 920 and 1010 K. They show, on a logarithmic scale, the change in the concentration of a given product due to a factor of 3 increase in the forward and reverse rate constants. The figures concentrate on reactions that have the most influence on the production rates of these species (at least an effect of 15%).

Concentrations of products which are formed by unimolecular decompositions are sensitive to fewer steps than concentrations of those which are associated with free radical reactions. Thus,

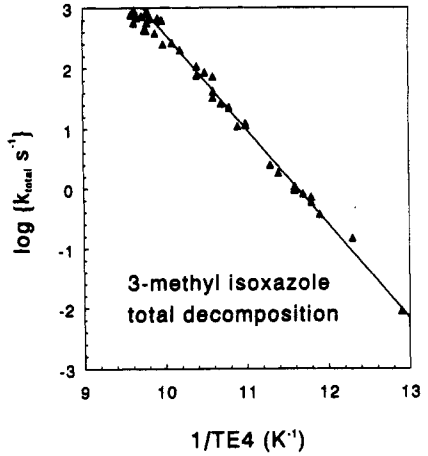

Figure 12. First-order rate constant for the overall decomposition of 5-methylisoxazole, calculated from the relation $k_{total} = -\ln\{[5\text{-methylisoxazole}]_t/[5\text{-methylisoxazole}]_0\}/t$. Its value is $k_{total} = 10^{18.46} \exp(-73 \times 10^3/RT)$ s^{-1}.

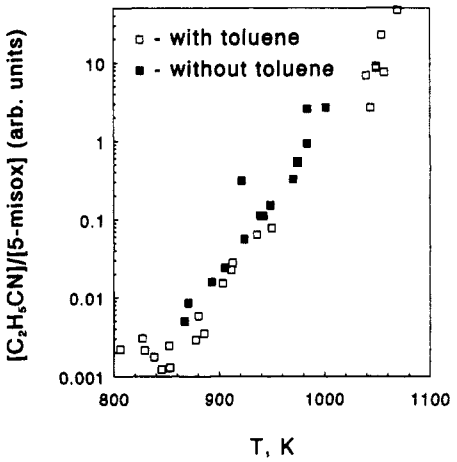

Figure 13. Logarithm of the ratio of the GC peak areas of propionitrile to that of 5-methylisoxazole is plotted against reciprocal temperature for experiments with and without toluene. No difference is seen between the two series of experiments, suggesting a unimolecular formation of propionitrile.

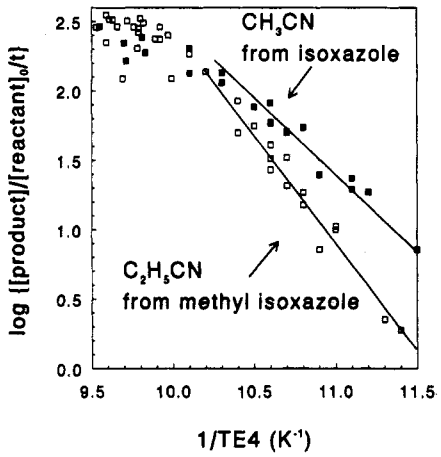

Figure 14. Comparison between the first-order rate constants of formation of acetonitrile in isoxazole and propionitrile in 5-methylisoxazole. The Arrhenius parameters of these two processes differ markedly.

propionitrile (Figure 3) and carbon monoxide (Figure 4) are mainly sensitive to reaction 1. An increase in the rate of reaction 2 which is the initiation for free radicals increases also the concentration of CO due to $CH_3CO \rightarrow CH_3 + CO$ (3). The rate of the latter is determined by the rate of reaction 2 so that the production rate of CO is independent of k_3.

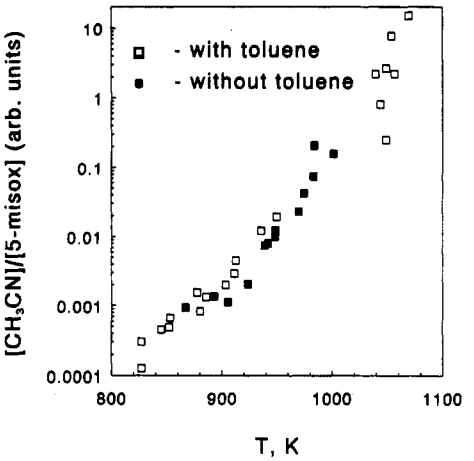

Figure 15. Logarithm of the ratio of the GC peak areas of acetonitrile to that of 5-methylisoxazole is plotted against reciprocal temperature for experiments with and without toluene. No clear effect of toluene can be observed.

Whereas the agreement between the experimental and calculated production rate of ethane (Figure 6) is very good, the agreement for methane is rather poor mainly in terms of the slope. We cannot provide a good explanation for this discrepancy except that there might be another channel that generates methane with methyl radicals not being the precursors.

The dashed lines drawn on the bottom left corner of Figures 5 and 6 are the simulated first-order rate constants for the production of methane and ethane, where the only source for free radicals are reactions 10 and 35. As can be seen, the concentrations of methyl radicals and H atoms generated by reactions 10 and 35 alone are too small to account for the concentration of ethane, methane, and other products whose formations depend upon the concentration of free radicals in the system.

Conclusion

Production rates and distribution of products obtained in the thermal decomposition of 5-methylisoxazole are successfully simulated with a kinetic scheme containing 23 species and 34 elementary reactions. The general agreement for most of the products (except for methane) as shown in Figures 3–11 seems to be satisfactory. A very important feature in the dissociation of 5-methylisoxazole is the very high preexponential factors and activation energies. These high preexponential factors indicate that very loose transition states, compatible with biradical structures, are obtained in the unimolecular dissociations of the reactant molecule. This behavior is completely different from the one found for the decomposition of isoxazole where a very stiff transition state is obtained.

Acknowledgment. This research was supported by a Grant from the G.I.F., the German–Israeli Foundation for Scientific Research and Development. We thank Professor P. Roth, who served as the cooperative investigator for this research, for his advice and encouragement.

References and Notes

(1) Lifshitz, A.; Wohlfeiler, D. *J. Phys. Chem.* **1992**, *96*, 4505.
(2) Lifshitz, A.; Bidani, M.; Bidani, S. *J. Phys. Chem.* **1986**, *90*, 5373.
(3) Tsang, W.; Lifshitz, A. *Annu. Rev. Phys. Chem.* **1990**, *41*, 559.
(4) Tsang, W. In *Shock Waves in Chemistry*; Lifshitz, A., Ed.; Marcel Dekker: New York, 1981.
(5) Westly, F.; Herron, J. T.; Cvetanovic, R. J.; Hampson, R. F.; Mallard, W. G. NIST Chemical Kinetics Data Base 17.
(6) Frank, P.; Braun-Unkhoff, M. *Proc. 16th Int. Symp. Shock Tubes Waves* **1987**, 83.
(7) Stull, D. R.; Westrum, Jr., E. F.; Sinke, G. C. *The Chemical Thermodynamics of Organic Compounds*; John Wiley & Sons: New York, 1969.
(8) Tsang, W.; Hampson, R. F. *Phys. Chem. Ref. Data* **1986**, *15*, 1087.
(9) Pedley, J. B.; Taylor, R. D.; Kirby, S. P. *Thermochemical Data of Organic Compounds*; Chapman and Hall: London, 1986.
(10) Stein, S. E.; Rukkers, J. M.; Brown, R. L. *NIST Stand. Ref. Data* **1991**, *25*.